Coupling between Translational Diffusion of a Solute and Dynamics of the Heterogeneous Structure: Higher Alcohol and Ionic Liquid

*Tsuyoshi Yamaguchi**

Graduate School of Engineering, Nagoya University, Chikusa, Nagoya, 464–8603, Japan

Tel: +81-52-789-3592

E-mail: yamaguchi.tsuyoshi@material.nagoya-u.ac.jp

ABSTRACT

Translational diffusion of nonpolar monoatomic solutes in a room-temperature ionic liquid and 1-octanol was studied by molecular dynamics simulation. The diffusion coefficient was evaluated in two different ways: (1) from the mean-square displacement of a freely diffusing solute; and (2) from the time correlation function of force acting on a fixed solute. The diffusion of free solute is much greater than the prediction of the Stokes–Einstein (SE) relation when the size of the solute is small, as has been reported by many experimental works. By contrast, the friction on fixed small solutes follows the SE relation. The mechanism of the solute diffusion in both solvents was then analyzed based on the coupling between the translational motion of the solute and the collective dynamics of the heterogeneous intermediate-range structure characteristic to these solvents. Analysis revealed that the coupling is present in all systems, but the relaxation is fast in the cases of free and small solutes. This suggests that the coupling can relax through the motion of the solute when the solute is free and small, while the relaxation of the heterogeneous structure itself is required for large or fixed solutes. The difference in the relaxation dynamics of the friction on the solute and the shear viscosity is explained as the coupling with different dynamic modes of the solvent. Therefore, the validity of the SE relation may not be a good criterion to judge whether the mechanisms of the diffusion and the viscosity are the same or not.

1. INTRODUCTION

Translational diffusion is one of the fundamental processes in solution chemistry—it directly governs the rates of diffusion-limited reactions, solvent extraction, and so on. In addition, it has been regarded as a microscopic probe to study solute–solvent interaction.

The Stokes–Einstein (SE) relation,

$$D = \frac{k_B T}{3\pi\sigma\eta}, \tag{1}$$

works as a first approximation for the translational diffusion coefficient, D, of an ordinary solute molecule, where D is reciprocally proportional to the diameter of the solute, σ, and the shear viscosity of the solvent, η. The symbols in the numerator, k_B and T, denote the Boltzmann constant and the absolute temperature, respectively. The SE relation was derived by hydrodynamic theory, in which a spherical solute is placed in a viscous continuum fluid. The coefficient 3π stems from the stick boundary condition at the surface of the solute, and it is replaced with 2π for the slip case.

The SE relation states that the diffusion coefficient is governed by the shear viscosity of bulk solvent. Considering that the shear viscosity is determined by the collective dynamics of neat solvent, the SE relation can be interpreted as that the translational motion is coupled to the collective solvent dynamics in some ways.

There are many dynamic modes in molecular liquids, and the collective mode that governs the viscosity varies among liquids. For example, the relaxation of the intermediate scattering function at the main peak of the static structure factor gives the viscoelastic relaxation of model liquids composed of monoatomic molecules;[1, 2] a similar relation is often found for many molecular liquids.[3] The collective reorientational relaxation plays an important role in the viscosity of liquids composed of molecules of

highly anisotropic shape.[4, 5] The dynamics of the intermediate-range structure gives the slowest mode of the viscoelastic relaxation of liquid higher alcohols.[4, 6] Therefore, one may consider that the validity of the SE relation depends on whether the shear viscosity and the solute diffusion are coupled to the same collective mode or not.

In recent work, we performed molecular dynamics (MD) simulation on a monoatomic solute in 1-octanol, where we changed the diameter of the solute from 2 to 12 Å.[7] The diffusion of the largest solute was comparable to the SE relation, while that of the smallest solute was about an order of magnitude faster than the SE relation, as has been reported experimentally by Evans and coworkers.[8, 9] The memory function was then calculated from the mean-square displacement based on the generalized Langevin equation (GLE) formalism. The relaxation rate of the memory function of the largest solute was comparable to that of the viscoelastic relaxation, while the memory function of the smallest solute relaxed much faster than the viscoelastic relaxation. The change in the relaxation rate of the memory function with the solute size was thus in harmony with the validity of the SE relation.

Another interesting finding of our previous work was the effect of the spatial fixing of the solutes. The calculation of the time correlation function of the total force acting on a fixed solute is one of the representative methods to estimate the position-dependent diffusion coefficient in heterogeneous media such as membranes and polymer gels,[10] although it tends to underestimate the absolute value of the diffusion coefficient.[11-13] The fundamental approximation there is the replacement of the random force on a free solute with the total force on a fixed solute, as is described in detail in the next section. In 1-octanol, fixing the small solute causes strong retardation of its diffusion. The ratio of the diffusion coefficients obtained in the two different ways is >10 when the solute is as small

as 2 Å. On the other hand, the two diffusion coefficients are close to each other for the large solute of 12 Å. A surprising point is that the diffusion coefficients of the fixed solutes appear to follow the SE relation even when the solute size is as small as 2 Å.

In this work, we now apply the same methodology to the diffusion of monoatomic nonpolar solutes in a room-temperature ionic liquid (RTIL) with a long alkyl chain, 1-methyl-3-octylimidazolium bis(trifluoromethanesulfonyl) amide ([omim][TFSA]). The translational diffusion of a small nonpolar solute in RTILs has been intensively studied, out of both scientific and industrial interests, because it is directly involved in gas absorption and separation by RTIL. Experimental results show that the friction on a small nonpolar solute in RTILs is more than an order of magnitude smaller than the SE relation,[14-17] as reported by Evans and coworkers on higher alcohols.[8, 9]

Both RTILs with a long alkyl chain and higher alcohols possess a similarity in their liquid structures in that they exhibit heterogeneous structures composed of polar and nonpolar domains.[18] The presence of the heterogeneous structure has been observed as the presence of a pre-peak in X-ray or neutron scattering experiments.[19-21] The polar domain is composed of anions and the charged head groups of cations in RTILs, while the hydroxyl group constitutes the polar domain of higher alcohols. The alkyl chains expelled from the polar domain constitute the nonpolar domain in both liquids. Since small nonpolar solutes favor the nonpolar domain, the formation of the heterogeneous structure is expected to strongly affect their diffusion.

Although the heterogeneous structure in the intermediate spatial scale is common to both [omim][TFSA] and 1-octanol, it plays different roles in determining the shear viscosity of these liquids. In the case of 1-octanol, the slowest mode of the viscoelastic relaxation, which contributes to about half of the total shear viscosity, is assigned to the

dynamics of the heterogeneous structure.[4] By contrast, the coupling between the shear stress and the dynamics of the heterogeneous structure is rather weak, and the shear viscosity of [omim][TFSA] is dominated by the ionic dynamics within the polar domain.[22] Therefore, it is expected that the coupling between the translational diffusion of a solute and the dynamics of the heterogeneous structure will differ in terms of the validity of the SE relation.

The coupling between the translational motion of a solute and the dynamics of the heterogeneous structure was discussed in our previous work solely based on the time profile of the memory function.[7] In the present work, the coupling is analyzed in detail by evaluating the cross-correlation between the random or the total forces on the solute and the transient solvation structure. The analysis is applied to our previous MD simulation on a solute in 1-octanol in addition to solutions of the RTIL for the purpose of comparison between diffusion in these two solvents.

This paper comprises four sections. After this introductory section, theoretical formalisms and the computational methods used in this work are summarized in Sec. 2. The results are reported in the subsequent section, Sec. 3, together with discussion of the results. The paper concludes with a summary in Sec. 4.

2. THEORETICAL AND COMPUTATIONAL METHODS

2.1. Generalized Lanvegin equation for solute diffusion

In MD simulation, the translational diffusion coefficient of a solute is usually evaluated from the mean-square displacement as[23]

$$D = \frac{1}{6}\lim_{t\to\infty}\frac{d}{dt}\langle|\boldsymbol{r}_X(t) - \boldsymbol{r}_X(0)|^2\rangle, \tag{2}$$

or from the velocity autocorrelation function as

$$D = \frac{1}{3}\int_0^\infty dt\,\langle\dot{\boldsymbol{r}}_X(0)\cdot\dot{\boldsymbol{r}}_X(t)\rangle. \tag{3}$$

Here, the position of the solute at time *t* is denoted as $\boldsymbol{r}_X(t)$. These two representations are equivalent to each other.

In statistical mechanics, on the other hand, the motion of the solute is often described by GLE as follows:[1, 24]

$$m\ddot{\boldsymbol{r}}_X(t) = -\int_0^t d\tau\gamma_R(t-\tau)\dot{\boldsymbol{r}}_X(\tau) + \boldsymbol{R}(t), \tag{4}$$

where *m* stands for the mass of the solute. The memory function, $\gamma_R(t)$, is related to the time correlation function of the random force, $\boldsymbol{R}(t)$, by the fluctuation–dissipation theorem as

$$\gamma_{\mathrm{R}}(t) = \frac{1}{3k_BT}\langle\boldsymbol{R}(0)\cdot\boldsymbol{R}(t)\rangle. \tag{5}$$

The diffusion coefficient can be described in terms of the time integral of the memory function as

$$\Gamma_{\mathrm{R},0} \equiv \int_0^\infty dt\,\gamma_R(t), \tag{6}$$

$$D = (k_BT)/\Gamma_{\mathrm{R},0}, \tag{7}$$

which is also equivalent to eqs. (2) and (3).

Instead of following the trajectory of a freely diffusing solute, Marrink and Berendsen proposed to estimate the position-dependent diffusion coefficient of a solute in heterogeneous media from the time correlation function of the total force on a spatially fixed solute (the MB method).[10] In their method, the random force $\boldsymbol{R}(t)$ is replaced with the total force, $\boldsymbol{F}(t)$, as

$$\gamma_{\mathrm{F}}(t) = \frac{1}{3k_BT}\langle \boldsymbol{F}(0) \cdot \boldsymbol{F}(t) \rangle \tag{8}$$

and the diffusion coefficient is obtained through the modification of eqs. (6) and (7) as

$$\Gamma_{\mathrm{F},0} \equiv \int_0^\infty dt\, \gamma_F(t), \tag{9}$$

$$D = (k_BT)/\Gamma_{\mathrm{F},0}. \tag{10}$$

The comparison of eqs. (7) and (10) with the SE relation, eq. (1), shows that $\Gamma_{\mathrm{R},0}$ and $\Gamma_{\mathrm{F},0}$ are equal to $3\pi\sigma\eta$ in the SE theory. By contrast, the Kubo–Green theory gives the shear viscosity in terms of the shear stress, P_{xy}, as[24, 25]

$$\eta = \frac{V}{k_{\mathrm{B}}T}\int_0^\infty dt\, \langle P_{xy}(0)P_{xy}(t)\rangle, \tag{11}$$

where V denotes the volume of the system. Therefore, both the friction coefficient and the shear viscosity are given by the time integrals of the random force and the shear stress, respectively.

2.2. Coupling between the translational motion of a solute and the solvation structure

The frictional force on a solute is a response of the solvent to the motion of the solute, which is caused by the distortion of the solvation structure around the diffusing solute. It is thus important to realize how the solvation structure is distorted in order to obtain a microscopic picture of solute diffusion.

The equilibrium solvation structure around a spherical solute of infinite dilution is characterized by the radial distribution function, $g_\alpha(r)$, defined as

$$g_\alpha(|\boldsymbol{r}|) \equiv \frac{1}{\rho_\alpha}\langle \rho_\alpha^{(2s)}(\boldsymbol{r})\rangle, \tag{12}$$

$$\rho_\alpha^{(2s)}(\boldsymbol{r}) \equiv \sum_{i\in\alpha} \delta(\boldsymbol{r}_i - \boldsymbol{r}_X - \boldsymbol{r}), \tag{13}$$

where ρ_α stands for the number density of the site α of bulk solvent. The superscript "(2s)" means that it involves the positions of two sites, one of which belongs to the solute. According to eq. (12), $\rho_\alpha^{(2s)}(\boldsymbol{r})$ gives the instantaneous solvation structure, whose statistical average yields the equilibrium solvation structure.

The coupling between the translational diffusion of a free solute and the dynamics of its solvation structure is analyzed using the cross-correlation function between $\boldsymbol{R}(t)$ and $\rho_\alpha^{(2s)}(\boldsymbol{r})$, defined as[26]

$$\frac{z}{|\boldsymbol{r}|}\rho_{R,\alpha}^{(2s)}(|\boldsymbol{r}|,t) \equiv \langle R_z(t)\rho_\alpha^{(2s)}(\boldsymbol{r})\rangle. \tag{14}$$

Inheriting the symmetry of $R_z(t)$, the right-hand side of eq. (14) possesses the *p*-type angular symmetry. The factor $\frac{z}{|\boldsymbol{r}|}$ on the left-hand side is thus introduced to factor out the trivial angular dependence. Although the time correlation function including the random force cannot be evaluated directly in MD simulation, it can be calculated from the cross-correlation function between $\rho_\alpha^{(2s)}(\boldsymbol{r})$ and the displacement of the solute, $\langle\{\boldsymbol{r}(t)-\boldsymbol{r}(0)\}\rho_\alpha^{(2s)}(\boldsymbol{r})\rangle$, using GLE, eq. (4), as

$$\int_0^t d\tau\,\langle R_z(\tau)\rho_\alpha^{(2s)}(\boldsymbol{r})\rangle = m_X\frac{d}{dt}\langle\{\boldsymbol{r}_z(t)-\boldsymbol{r}_z(0)\}\rho_\alpha^{(2s)}(\boldsymbol{r})\rangle$$

$$+\int_0^t d\tau\gamma_R(t-\tau)\langle\{\boldsymbol{r}_z(\tau)-\boldsymbol{r}_z(0)\}\rho_\alpha^{(2s)}(\boldsymbol{r})\rangle. \tag{15}$$

The counterpart of eq. (14) for a fixed solute is given by replacing $\boldsymbol{R}(t)$ with $\boldsymbol{F}(t)$ as follows:

$$\frac{z}{|\boldsymbol{r}|}\rho_{F,\alpha}^{(2s)}(|\boldsymbol{r}|,t) \equiv \langle F_z(t)\rho_\alpha^{(2s)}(\boldsymbol{r})\rangle, \tag{16}$$

Direct evaluation is possible in MD simulation.

2.3. Linear response picture for the calculation schemes of diffusion coefficient

In this subsection, we present physical pictures for the two different methods to calculate the diffusion coefficients based on the linear response theory in order to discuss the origin of their differences.

The friction coefficient on a solute is defined as the proportionality coefficient between the velocity of the solute and the force acting on it. There are two different ways to obtain the proportionality coefficient in nonequilibrium MD simulation. The first is to calculate the average velocity by dragging the solute with a constant force, and the second is to calculate the average force by dragging the solute at a constant velocity. Hereinafter, we show that, in the linear response limit, the first one reduces to the calculation from the mean-square displacement of a free solute, while the second one is to that from the force–force correlation function of a fixed solute.

In the linear response theory, the perturbation on the system is described as the additional term in the Hamiltonian, $\epsilon H'$, where ϵ is a small real constant, and H' is assumed to be time-independent, for simplicity. After the perturbation is turned on at t = 0, the average of the physical quantity A at $t = \tau$ is given by

$$\langle A(\tau)\rangle_{ne} = -\frac{\epsilon}{k_B T}\int_0^\tau dt\, \langle A(0)\dot{H}'(t)\rangle_{eq}, \tag{17}$$

where the angular brackets with the suffixes "ne" and "eq" stand for the ensemble averages with and without the perturbation, respectively. Here, the equilibrium averages of A and H' in the absence of the perturbation are assumed to be zero, for simplicity.

In the first case, where the solute is dragged in the z-direction with a constant force F_z, the observed quantity is $A = \dot{r}_{X,z}$ and the perturbation Hamiltonian is $H' = -F_z r_{X,z}$. Their substitution into eq. (17) gives

$$\langle \dot{r}_{X,z}(\infty)\rangle_{ne} = \frac{F_z}{k_B T}\int_0^\infty dt\, \langle \dot{r}_{X,z}(0)\dot{r}_{X,z}(t)\rangle, \tag{18}$$

which results in the expression of D in terms of the velocity autocorrelation function, eq. (3).

Next, we consider the second case in which the solute is dragged in the z-direction at the constant velocity, $\dot{r}_{X,z} \equiv v_0$. Within the linear response scheme, the response to the constant velocity at $t > 0$ is equal to the response integrated over the whole time to the solute velocity whose time profile is the δ-function at $t = 0$, $\dot{r}_{X,z}(t) \equiv v_0\delta(t)$. Such a time profile of the solute velocity is actually equivalent to the infinitesimal v_0 displacement of the solute in the z-direction at $t = 0$.

The spatially fixed solute can be regarded as an external potential on the solvent, $U_{\mathrm{uv}}(\{\boldsymbol{r}_i\}; \boldsymbol{r}_X)$, where U_{uv} stands for the solute–solvent interaction. The displacement of the solute thus results in the perturbation as

$$U_{\mathrm{uv}}(\{\boldsymbol{r}_i\}; \boldsymbol{r}_X + v_0\hat{\boldsymbol{z}}) - U_{\mathrm{uv}}(\{\boldsymbol{r}_i\}; \boldsymbol{r}_X) \simeq v_0 \frac{\partial}{\partial r_{X,z}} U_{\mathrm{uv}}(\{\boldsymbol{r}_i\}; \boldsymbol{r}_X) = -v_0 F_{X,z}, \quad (19)$$

which works as the perturbation Hamiltonian. Therefore, the response of $F_{X,z}$ to $\dot{r}_{X,z}(t) \equiv v_0\delta(t)$ is given by

$$\langle F_{X,z}(t)\rangle_{ne,\delta} = -\frac{v_0}{k_BT}\langle F_{X,z}(0)F_{X,z}(t)\rangle_{eq}, \quad (20)$$

where δ in the suffix means the response to $\dot{r}_{X,z}(t) \equiv v_0\delta(t)$. The response to the constant velocity, $\langle F_{X,z}(t)\rangle_{ne,v_0}$, is obtained by integrating eq. (20) over t as

$$\langle F_{X,z}(t)\rangle_{ne,v_0} = -\frac{v_0}{k_BT}\int_0^\infty dt\, \langle F_{X,z}(0)F_{X,z}(t)\rangle_{eq}. \quad (21)$$

The expression of the diffusion coefficient in the MB method, eqs. (8)–(10), is obtained from eq. (21).

The replacement of $F_{X,z}(t)$ in eq. (20) with $\rho_\alpha^{(2s)}(\boldsymbol{r}, t)$ gives

$$\langle \rho_\alpha^{(2s)}(\boldsymbol{r}, t)\rangle_{ne,\delta} - \langle \rho_\alpha^{(2s)}(\boldsymbol{r}, t)\rangle_{eq} = -\frac{v_0}{k_BT}\langle F_{X,z}(0)\rho_\alpha^{(2s)}(\boldsymbol{r}, t)\rangle_{eq}, \quad (22)$$

which means that $\rho_{F,\alpha}^{(2s)}(r,t)$ defined by eq. (16) describes the anisotropic change in the solvation structure after the infinitesimal displacement of the fixed solute. Its integration over the whole time thus describes the distortion of the solvation structure around the solute moving in a constant velocity. In a similar way, it can be shown that $\rho_{R,\alpha}^{(2s)}(r,t)$ is related to the anisotropic change in the solvation structure around a free solute after the application of an infinitesimal impulsive force, although the derivation is not shown here for brevity.

2.4. Computational details

The MD simulation was performed on systems composed of a nonpolar solute and 1000 ion pairs of [omim][TFSA]. The molecules are confined within a cubic cell with periodic boundary conditions. The temperature and the pressure of the system are 353 K and 1 bar, respectively, controlled using the Nosé–Hoover and the Parrinello–Rahman methods. The united atom model proposed by Zhong and coworkers was employed for [omim][TFSA], in which the total charges of the ions are scaled to be ±0.8*e*.[27] The solute is a Lennard–Jones (LJ) sphere, whose parameters (except for the diameter) are equal to those of argon.[28] The LJ diameter of the solute, σ_{LJ}, was changed as follows: 2, 3.4, 6, 8, and 12 Å.

The equation of motion was integrated using the leapfrog algorithm with a time step of 1 fs. The systems were equilibrated for 100 ns prior to the production run of 1 μs length. The production runs were performed twice for each condition, and their averages are presented as the final results. The bond lengths involving a hydrogen atom were fixed using the LINCS algorithm;[29] other bond lengths, bond angles, and dihedral angles were

treated as flexible. The long-range part of the Coulombic interaction was handled using the particle mesh Ewald (PME) method, and the short-range parts were cut off at 1.2 nm. The center-of-mass velocity of the whole system was shifted to be zero at each 100 fs in the cases of both free and fixed solutes. The roles of the center-of-mass velocity shift are different in the systems of free and fixed solutes.[13] It is introduced to compensate the incomplete momentum conservation in the PME calculation in the former, whereas it works as a momentum sink at the infinite distance in the latter. The shift interval for the fixed-solute system was confirmed to be small enough according to the criteria we have proposed in our previous work.[13] All the MD simulation runs were performed using the GROMACS software package,[30] and homemade programs were used for the analysis of the trajectories.

The MD simulations on the solutions of an LJ solute in 1-octanol were performed in our previous work,[7] and their trajectories were further analyzed in this work. The simulation conditions were similar to those for [omim][TFSA] solutions in this work, with details described in our previous paper.[7] Briefly, the systems were composed of an LJ solute and 1000 solvent molecules. The temperature and the pressure were 298 K and 1 bar, respectively. The TraPPE-UA model was used for 1-octanol,[31, 32] and all the bond lengths were fixed using the LINCS algorithm. The diameter of the solute was changed as follows: 2, 3.4, 6, 8, and 12 Å. Other parameters for the solutes were the same as those for argon. The production runs of 1 μs were performed twice for each set of conditions.

The shear viscosity and the viscoelastic relaxation of neat solvents were also taken from our previous MD simulation works.[4, 22]

3. RESULTS AND DISCUSSION

3.1. Equilibrium structure

Prior to addressing the dynamics of the solutes and the solvation structure, we show the radial distribution functions of the solvent sites around the solutes in Fig. 1 in order to provide pictures of the equilibrium solvation structure. The radial distribution functions in [omim][TFSA] and 1-octanol are shown in Fig. 1a and 1b, respectively. In both figures, the functions of both the smallest and the largest solutes in this work, σ_{LJ} = 2 and 12 Å, respectively, are plotted. The averages of the distributions around the free and the fixed solutes are plotted in Fig. 1. There are no meaningful differences between the results with and without the positional constraint.

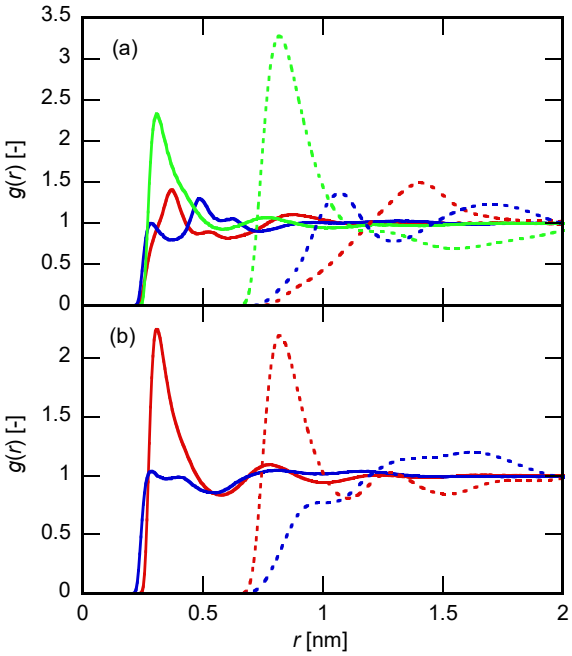

Figure 1. The radial distribution functions, $g(r)$, of the solvent sites around a solute in (a) [omim][TFSA] and (b) 1-octanol. Distribution functions around the solutes of σ_{LJ} = 2 and 12 Å are shown by the solid and the dotted curves, respectively. In (a), the distributions of the algebraic center of the five atoms of the imidazolium ring of the omim cation, the nitrogen site of the TFSA anion, and the terminal methyl site of the octyl chain of the

omim cation are shown by the red, blue, and green curves, respectively. In (b), the distributions of the methyl and the oxygen sites are shown by the red and blue curves, respectively.

The molecular structure of RTIL with a long alkyl chain is composed of three groups, namely, the anion, the charged head group of the cation, and the nonpolar alkyl chain of the cation. In this work, the position of the anion is represented by the central nitrogen atom of the TFSA anion, that of the charged head group of the omim cation by the algebraic center of the five atoms of the imidazolium ring, and that of the alkyl chain by its terminal methyl group.

In Fig. 1a, the large distributions of the methyl group are found at the contact distances of both the small and the large solutes, indicating that the nonpolar solutes favor the nonpolar domain. The situation is similar in 1-octanol, as the large distribution of the methyl group is also observed in Fig. 1b.

The characteristics of the solvation structures exhibited in Fig. 1 are related to the structure of the respective neat solvents. Their X-ray static structure factors were calculated in our previous works,[4, 22] and plotted together in Fig. 2. Both solvents show peaks at 3~4 nm^{-1} and ~14 nm^{-1}. The former, called "pre-peak", originates in the characteristic heterogeneous structure composed of polar and nonpolar domains, and the latter describes the molecular packing common to other molecular liquids. In addition, [omim][TFSA] exhibits a peak at 8 nm^{-1}, which is assigned to the charge-alternation structure made by the anion and the head group of the cation. [33]

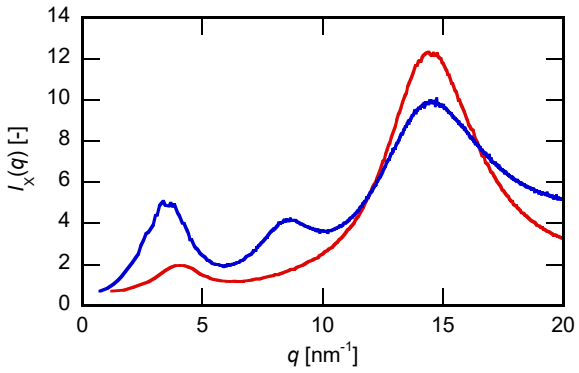

Figure 2. The X-ray static structure factors of neat 1-octanol (red) and [omim][TFSA] (blue) calculated in our previous MD simulation studies.[4, 22] Their amplitudes are scaled by arbitrary factors to improve the visibility.

In both solvents and around both solutes, the depletion of the methyl groups and the excess distribution of the polar groups are found in their solvation structures in Fig. 1 at about 0.8 nm distant from the first contact peaks of the methyl groups. Around the largest solute, for example, the first peak of the methyl group exists at r = 0.8 nm. At r = 1.5~1.6 nm, the distribution of the methyl group exhibits shallow basin in both solvents, and the broad peaks of the charged groups and oxygen atom lie at the same position. The long-range alternating structure of the contrast between the polar and the nonpolar groups around the solutes thus means that the solvation of the nonpolar solutes is coupled to the heterogeneous structures characteristic to these solvents represented by the pre-peaks shown in Fig. 2.

In [omim][TFSA], the anion distributes closer to the solute than the cation head group, as is shown in Fig. 1a, probably because of the smaller size of the former. The antiphase oscillations of the anion and the cationic head group are imposed on the distribution functions of these sites at larger distances, and the period of the oscillation is shorter than

that of the methyl group. This means that the solvation of the nonpolar solutes is also coupled to the charge-alternation structure, which is also characteristic to the structure of RTIL.[33]

3.2. Diffusion coefficient and validity of SE relation

The SE relation, eq. (1), defines the hydrodynamic diameter of the solute, σ_{H}, from its diffusion coefficient as

$$\sigma_H = \frac{k_{\mathrm{B}}T}{3\pi\eta D}, \tag{23}$$

which describes the effective diameter of the solute in terms of its mobility. The values of σ_{H} for the solutes in [omim][TFSA] are plotted in Fig. 3 as the function of σ_{LJ}. These two diameters are equal to each other when the SE relation with the stick boundary condition holds, whereas $\sigma_H = \frac{2}{3}\sigma_{LJ}$ is expected for the slip boundary condition. These two relationships are also shown in Fig. 3, as the solid and the dashed lines, respectively. The effects of the finite system size on the diffusion coefficient were corrected using the formula proposed by Yeh and Hummer as[34]

$$D_\infty = D_{MD} + \frac{2.837\,297}{6\pi\eta L}, \tag{24}$$

where the diffusion coefficients before and after the correction are denoted as D_∞ and D_{MD}, respectively, and L stands for the size of the cubic simulation cell. The values of σ_{H} before and after the correction are plotted with the filled and the open symbols, respectively, indicating that the system size effect is negligible for our present discussion. The results obtained with 1-octanol have been published in our previous paper, in the same format.[7]

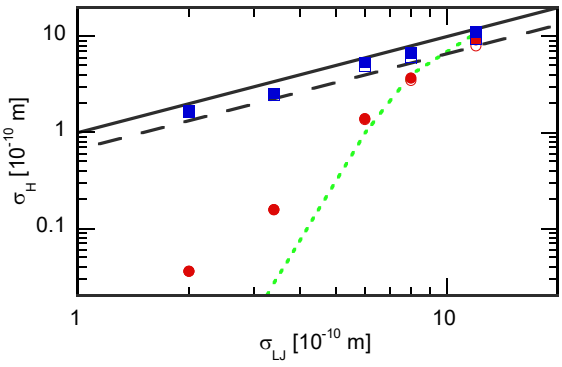

Figure 3. The hydrodynamic diameters of the solutes, σ_H, plotted against the LJ diameter, σ_{LJ}. Results of the free and the fixed solutes are shown by the red circles and the blue squares, respectively, and the values before and after the system size correction are shown by the corresponding filled and open symbols, respectively. The black solid line indicates the SE relation with the stick boundary condition, $\sigma_H = \sigma_{LJ}$, and the black dashed line does likewise with the slip boundary, $\sigma_H = \frac{2}{3}\sigma_{LJ}$. The green dotted curve shows an empirical equation that correlates various experimental results in RTILs.[15]

According to Fig. 3, the application of the MB method has little effect on the diffusion coefficient of the largest solute, σ_{LJ} = 12 Å. The difference between these two methods, that is, free and fixed solutes, increases with decreasing solute size, and the friction coefficient of the free solute becomes nearly two orders of magnitude larger than that of the fixed one in the case of σ_{LJ} = 2 Å. The free and small solutes diffuse much faster than the prediction of the SE relation, whereas the fixed solutes approximately follow the hydrodynamic SE relation. All these trends are in common with those of solute diffusion in 1-octanol, as reported in our previous paper.[7] Upon comparing the results in [omim][TFSA] and 1-octanol, we note that the deviation of the diffusion of free solutes from the SE relation is more significant in the case of the former.

Kaintz and coworkers proposed an empirical equation that describes the deviation of the experimental diffusion coefficients of small nonpolar solutes in RTIL from the SE relation.[15] This is also plotted in Fig. 3, with the green dotted curve, to compare our MD simulation with experiments. Their empirical equation contains the molecular volumes of both solute and solvent. The volume of [omim][TFSA] was taken from their work, and the volume of the sphere of σ_{LJ} diameter was used for the solute. As is demonstrated in Fig. 3, the agreement between the MD simulation of free solute and the empirical equation is almost quantitative, though the simulation underestimates the deviation from the SE relation for smaller solutes. Therefore, we consider that our MD simulation with free solutes describes the experimental results of translational diffusion of nonpolar solutes in RTILs at least qualitatively.

3.3. Memory function and viscoelastic relaxation

The running integral of the memory functions, defined as

$$\Gamma_X(t) \equiv \int_0^t d\tau\, \gamma_X(\tau) \quad (\mathrm{X} = \mathrm{R}, \mathrm{F}), \tag{25}$$

of solutes in [omim][TFSA] are normalized to the values at $t \to \infty$, $\Gamma_{R,0}$ and $\Gamma_{F,0}$, and shown in Fig. 4 for the analysis of dynamics coupled to the diffusion of the solute. The results of the free and the fixed solutes are exhibited in Fig. 4a and 4b, respectively. In both figures, the running integral of the time correlation function of the shear stress,

$$\eta(t) = \frac{V}{k_B T} \int_0^t d\tau\, \langle P_{xy}(0) P_{xy}(\tau) \rangle, \tag{26}$$

is also plotted, for comparison. The corresponding plots for the solutes in 1-octanol are not shown here; they are included in our previous paper.[7]

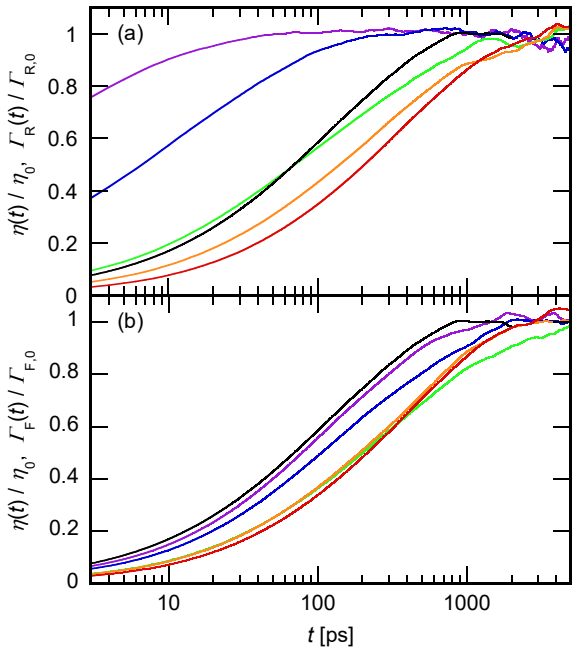

Figure 4. The normalized running integral of (a) free solutes and (b) fixed solutes in [omim][TFSA]. The sizes of the solutes are 2 (purple), 3.4 (blue), 6 (green), 8 (orange), and 12 Å (red). The normalized running integral of the time correlation function of shear stress, $\eta(t)$, defined by eq. (26), is also plotted by black curve in both panels, for comparison.

The relaxation of the memory function of the free solutes strongly depends on the solute size, as is demonstrated in Fig. 4a. The relaxation is almost complete within 50 ps in the case of the smallest solute (2 Å), whereas in the case of the largest solute (12 Å) it takes about 5 ns. The fast relaxation of the small solute is consistent with the large diffusion coefficient, because the fast relaxation means a small integrated friction. Although the dependence of the relaxation rate on the solute size is also observed in the fixed-solute case (Fig. 4b), the variation of the relaxation rate is much smaller. Since the initial values of the memory functions of the free and the fixed solutes are equal to each other, their

differences in the time-integrated friction should be ascribed to that in the relaxation time. Upon comparing the memory functions of the free and the fixed solutes of the same size, we note that they are close to each other for the largest solute, which is in harmony with their similar diffusion coefficients, shown in Fig. 3. On the other hand, fixing the solute significantly retards the relaxation of the memory function of the smallest solute, which is the reason for the large change in the diffusion coefficient. All the properties above are common to the results already published for the solute diffusion in 1-octanol.[7]

A large difference is found, however, between [omim][TFSA] and 1-octanol solutions in terms of the relationship between the relaxations of the random force on the solute and the shear stress. In 1-octanol, the relaxation of the memory function of the largest solute is as slow as the viscoelastic relaxation. On the other hand, the memory function of the largest solute in [omim][TFSA] relaxes more slowly than the viscoelastic relaxation of the solvent, as is exhibited in Fig. 4a and 4b.

3.4. Coupling between random force and solvation structure

The cross-correlation functions between the random force and the transient solvation structure, defined by eqs. (14) and (15), are now analyzed to obtain a detailed picture on the frictional force felt by the solutes. The cross-correlation functions are plotted in the time-integrated form, because the integration over the whole time describes the anisotropy of the solvation structure around a solute dragged by a constant force or in a constant velocity according to the linear response picture given in Sec. 2.3. The negative sign in Eq. (22) means that the positive cross correlation describes the depletion of the distribution in the direction of the motion of the solute. Reciprocal relation also states that the solute is dragged toward the sites of positive cross correlation.

First, the results on the time integrals of the cross-correlation functions in 1-octanol are shown in Fig. 5, at various times. The sizes of the solutes are 2 and 12 Å. The results of both the free and the fixed solutes are plotted.

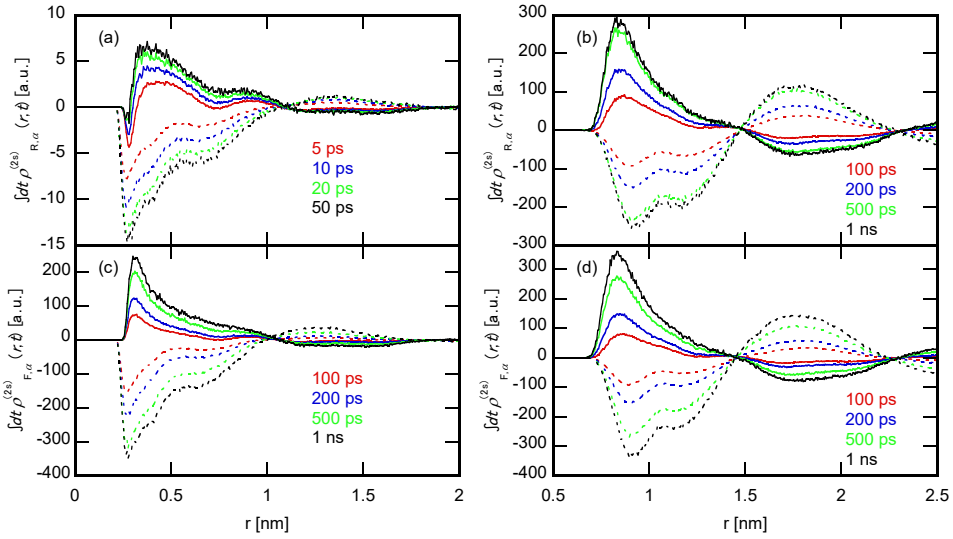

Figure 5. The cross-correlation functions between the random force and the transient solvation structure in 1-octanol integrated over time from 0 to *t*. The correspondence between the colors of the curves and the values of the upper limits of the time integral is shown in each panel. The solutes are (a) free, σ_{LJ} = 2 Å, (b) free, σ_{LJ} = 12 Å, (c) fixed, σ_{LJ} = 2 Å, and (d) fixed, σ_{LJ} = 12 Å. The distributions of the methyl group and the oxygen atom are shown by the solid and the dotted curves, respectively.

In all the panels of Fig. 5, irrespective of the solute size and whether the solute is free or fixed, a positive distribution of the methyl group and a negative one of the oxygen atom are observed around the solutes. The positive and the negative distributions of the methyl group and the oxygen atom mean that the solute is dragged toward the methyl group and expelled from the oxygen atom, which is consistent with the equilibrium radial distribution functions in Fig. 1a. The distributions of the methyl group and the oxygen

atom exhibit long-range oscillations, whose phases are opposite to each other. The wavelength of the oscillation is close to the size of the heterogeneous domain structure of the neat solvent. Therefore, Fig. 5 clearly indicates that the translational diffusion of the nonpolar solutes in 1-octanol are coupled to the characteristic polar–nonpolar heterogeneous structure.

The time-integrated distributions of both sites increase with time, and the increasing rate appears independent of sites. Compared with the memory functions reported in our previous paper,[7] the increasing rates are close to the relaxation rates of the memory functions of the corresponding solutes. In particular, the fast relaxation of the memory function of the free solute of σ_{LJ} = 2 Å is ascribed to the fast dynamics of its solvation structure.

Calculations of the cross-correlation functions were also performed for solutes in [omim][TFSA]. The time-integrated functions for σ_{LJ} = 2 and 12 Å in the free and fixed cases are shown in Fig. 6. The upper limits of the time integral were determined to be sufficiently large so that the integrals are converged.

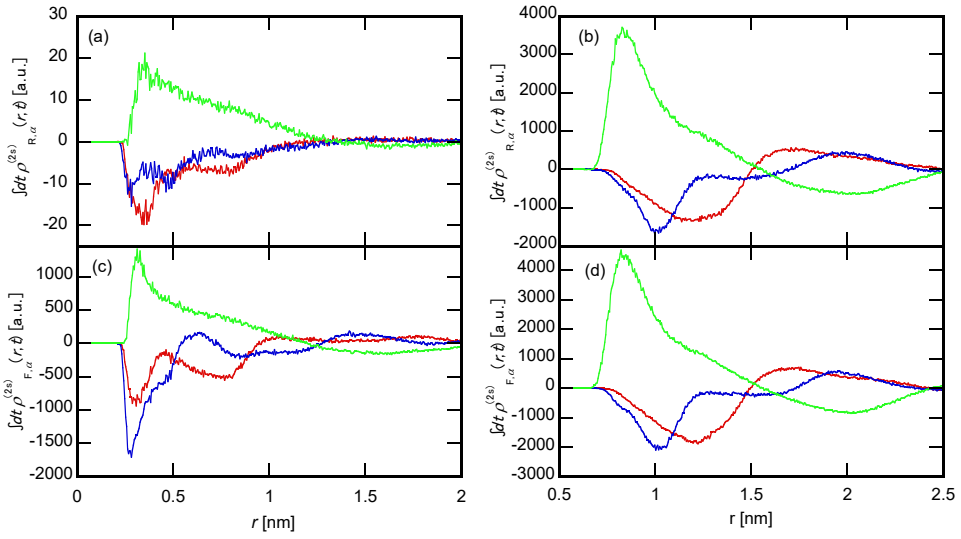

Figure 6. The cross-correlation functions between the random force and the transient solvation structure in [omim][TFSA] integrated over time. The solutes are (a) free, σ_{LJ} = 2 Å, (b) free, σ_{LJ} = 12 Å, (c) fixed, σ_{LJ} = 2 Å, and (d) fixed, σ_{LJ} = 12 Å. The distributions of the cation head group, the anion, and the methyl group of the octyl chain of the cation are shown by the red, blue, and green curves, respectively. The values of the upper limits of the time integrals are 200 ps for panel (a) and 5 ns for the other panels.

The characteristics of the time-integrated distributions in [omim][TFSA] shown in Fig. 6 are similar to those in 1-octanol shown in Fig. 5, in terms of the large positive distribution of the nonpolar site and the negative distribution of the polar sites in the vicinity of the solute. Both distributions show long-range oscillations, and the phases of the polar and nonpolar sites are opposite to each other. The wavelength of the antiphase oscillation of the polar and nonpolar groups corresponds to the scale of the heterogeneous structure of the neat solvent. Therefore, the diffusion of the nonpolar solute in [omim][TFSA] is also coupled to the heterogeneous structure of the solvent. Although the results are not shown here (for brevity), the relaxation of the distribution of the methyl group follows that of the corresponding memory function.

Here, a difference from the results in 1-octanol is that a small and shorter-range oscillation is imposed on the distributions of the polar groups, namely, the anion and the head group of the cation. The phases of the cation and the anion are opposite to each other, indicating that the diffusion of the solute is also coupled to the charge-alternation mode. Since the coupling with the charge-alternation mode is present even in the equilibrium structure (Fig. 1a), it is natural that the coupling is present in the translational diffusion.

Analysis of the cross-correlation between the random force and the transient solvation structure clearly demonstrates that the translational diffusion of nonpolar solutes is coupled to the intermediate-range heterogeneous structure in both 1-octanol and [omim][TFSA]. The coupling itself is easily understood in terms of the selective solvation of the solute by the nonpolar group, as demonstrated in Fig. 1. When the polar–nonpolar heterogeneous structure is present in the solvent, the mean force works on the nonpolar solute toward the nonpolar domain because the solute favors the nonpolar domain over the polar one. The relaxation of the mean force then follows that of the heterogeneous solvation structure around the solute. Therefore, the mean force on the fixed solute relaxes following the dynamics of the solvent around the solute. In the case of free solutes, the relaxation of the heterogeneous structure around the solute occurs through the relative motion between the solute and the solvents. Since small solutes can diffuse rapidly through the nonpolar domain, the solvation structure around the solute can relax through the motion of the solute itself, even though the heterogeneous structure of the solvent is frozen. This explains the fast relaxation of the memory function and the solvation structure around the small solute. The contribution of the solute motion decreases with increasing solute size. The dynamics of the solvation structure around the large solute is determined by the motion of the solvent, irrespective of the spatial constraint on the solute. In our previous paper, we found that the relaxation time of the memory function of free solutes in octanol is comparable to the time required for the solute to diffuse the distance corresponding to the wavenumber of the pre-peak,[7] which supports our idea described above.

The difference between the free and the fixed solutes can also be understood in terms of the linear response picture described in Sec. 2.3. Given that the nonpolar solute

disfavors the polar domain in both solvents, the polar domains can be regarded as randomly placed obstacles for the motion of the solute. The idea that regards the polar domains as an obstacle for the diffusion of nonpolar solutes is in harmony with the computational study of Araque and Margulis, i.e., that a nonpolar solute feels strong friction in the vicinity of the polar domain.[35] When a small solute is dragged by a constant force, it can avoid the obstacle and proceed forward even though the positions of the obstacles are fixed. By contrast, the solute moving with a constant velocity should feel strong resisting force upon encountering the obstacle when the obstacle is in its way. For large solutes, the voids between the obstacles are not large enough for the solute to move through, and the time required for the obstacles to avoid the solute to make way is important for the motions of solutes dragged by either constant force or by velocity.

Since the couplings between the diffusion of the solute and the dynamics of the heterogeneous structures are similar in both solvents considered here, the difference in the relationship between the memory function and the viscoelastic relaxation could be ascribed to the different origins of the latter. Experimental and computational studies have revealed that the slowest mode of the viscoelastic relaxation of higher alcohols, including 1-octanol, is ascribed to the dynamics of the heterogeneous structure.[4, 6] Since the same dynamics governs both the viscoelastic relaxation and the solute diffusion, it is natural for them to exhibit similar dynamics, as reported by us in our previous paper.[7] On the other hand, although the dynamics of the heterogeneous structure is also coupled to the viscoelastic relaxation of RTILs, its contribution to their steady-state shear viscosity is rather minor, and the main part of the viscoelastic relaxation is ascribed to the dynamics of the charge-alternation mode.[22] Then, the faster relaxation of the charge-alternation

mode compared with that of the intermediate-range heterogeneous structure explains why the memory function relaxes more slowly than the viscoelastic relaxation.

The remaining question is the validity of the SE relation in these two solvents. In 1-octanol, both the shear viscosity and the solute diffusion are coupled to the same dynamic mode of the solvent, namely, the dynamics of the heterogeneous structure, when the solute is large or fixed. Therefore, it is natural that the diffusion coefficient follows the shear viscosity as is presented by the SE relation under these conditions. In [omim][TFSA], however, the dynamic mode of the solvent coupled to the solute diffusion is different from that of the shear viscosity even though the solute is large or fixed. Hence, there seems to be no reason for the SE relation to hold, contrary to the results in Fig. 3 that support the validity of the SE relation. There must be a reason for the SE relation in [omim][TFSA] other than that both the diffusion and the shear viscosity are governed by the same microscopic dynamics. In other words, a mere comparison between the zero-frequency values of the shear viscosity and the diffusion coefficient alone cannot reveal whether these two dynamic quantities are determined by the same microscopic dynamics or not—the time or frequency dependence of these quantities gives valuable information on their microscopic origin.

Another issue to be treated in a future work is the extension of our analysis based on the cross correlation to other systems. The diffusion of small solutes in *n*-tetradecane shows similar decoupling from viscosity,[8, 9] although the degree of the decoupling is smaller than those in 1-octanol and [omim][TFSA], and we have succeeded in reproducing the decoupling in our previous work by MD simulation.[7] Since shear viscosity of liquid *n*-tetradecane is strongly coupled to the collective orientation, the analysis used in this work is not applicable directly to *n*-tetradecane.[4] We guess that the

function to be analyzed would be the cross correlation between the random force on a solute and the distribution of the chain orientation around the solute. The microscopic modes that govern the shear viscosity varies among liquids, and we need to define proper variables to be correlated with the random force on a solute depending on the mechanism of the shear viscosity of the solvent under consideration.

4. SUMMARY

The diffusion of a nonpolar monoatomic solute in an ionic liquid, [omim][TFSA], was studied by means of MD simulation as a function of both the LJ diameter and the positional constraint. The positional constraint enhances the friction on small solutes significantly, whereas its influence to large solutes is small. The diffusion of free and small solutes is much faster than the prediction of the SE relation, as has been reported experimentally, whereas the fixed solute follows the SE relation even if its size is much smaller than that of solvent ions. These trends are similar to those of solute diffusion in 1-octanol, reported in our previous paper.[7]

The memory function for the solute diffusion, i.e., the time-dependent friction coefficient, was also calculated from the MD simulation. The relaxation of the memory function of free solute becomes remarkably faster with decreasing solute size, whereas the change in the relaxation of the memory function of fixed solute with the solute size is relatively small. The variation of the relaxation rate is in harmony with that of the hydrodynamic diameter determined by the diffusion coefficient. This trend in [omim][TFSA] is common to that in 1-octanol. However, the relationship between the memory function and the viscoelastic relaxation in [omim][TFSA] is different from that in 1-octanol. The relaxation of the memory function of the solute of 12 Å diameter,

irrespective of the positional constraint, is several times slower than that of the viscoelastic relaxation in [omim][TFSA], whereas their relaxations are comparable to each other in 1-octanol.

The cross-correlation functions between the random force on the solute and the transient solvation structure were calculated in both solvents in order to analyze the coupling between the solute diffusion and the solvent dynamics. The analysis clearly demonstrates that the solute diffusion is coupled to the heterogeneous structure around the solute in both solvents, irrespective of the solute size and the positional constraint. The relaxation of the solvation structure around the free and small solutes occurs through the solute motion, whereas the motion of solvent molecules is required for fixed or large solutes.

The memory functions of the fixed or large solutes relax as slowly as the shear stress in 1-octanol because they are coupled to a similar dynamic mode of the solvent. The former is slower than the latter in [omim][TFSA] because the latter is governed by the charge-alternation mode whose relaxation is faster than that of the heterogeneous structure. The correspondence between the relaxation dynamics is thus easily understood in terms of the microscopic dynamic modes coupled to the diffusion and viscosity. However, the difference in the microscopic mechanism is not evident in the zero-frequency values of these two transport coefficients. The diffusion coefficients of fixed or large solutes follow the SE relation in both solvents in a similar way. This means that mere examination of the validity of the SE relation does not provide sufficient information on the microscopic mechanism of diffusion, whereas the time or frequency dependence of the diffusion coefficient and the shear viscosity, if available, offers a powerful probe into the microscopic mechanism.

ACKNOWLEDGMENT

We are grateful for financial support from Japan Society for the Promotion of Science (JSPS) KAKENHI (Grant Nos. 19H02677 and 19K03768).

Data Availability Statement

The data that support the findings of this study are available from the corresponding author upon reasonable request.

REFERENCES

(1) Balucani, U.; Zoppi, M. *Dynamics of the Liquid State*. Clarendon Press: Oxford, 1994.

(2) Yamaguchi, T. Stress-Structure Coupling and Nonlinear Rheology of Lennard-Jones Liquid. *J. Chem. Phys.* **2018,** *148*, 234507.

(3) Yamaguchi, T. Experimental Study on the Relationship between the Frequency-Dependent Shear Viscosity and the Intermediate Scattering Function of Representative Viscous Liquids. *J. Chem. Phys.* **2016,** *145*, 194505.

(4) Yamaguchi, T. Viscoelastic Relaxations of High Alcohols and Alkanes: Effects of Heterogeneous Structure and Translation-Orientation Coupling. *J. Chem. Phys.* **2017,** *146*, 094511.

(5) Yamaguchi, T.; Matsuoka, T. Translation-Orientation Coupling and Cox-Merz Rule of Liquid Hexane. *J. Chem. Phys.* **2018,** *149*, 204502.

(6) Yamaguchi, T.; Saito, M.; Yoshida, K.; Yamaguchi, T.; Yoda, Y.; Seto, M. Structural Relaxation and Viscoelasticity of a Higher Alcohol with Mesoscopic Structure. *J. Phys. Chem. Lett.* **2018,** *9*, 298-301.

(7) Yamaguchi, T. Decoupling between Solvent Viscosity and Diffusion of a Small Solute Induced by Self-Motion. *J. Phys. Chem. Lett.* **2021,** *12*, 7696-7700.

(8) Evans, D. F.; Tominaga, T.; Chan, C. Diffusion of Symmetrical and Spherical Solutes in Protic, Aprotic, and Hydrocarbon Solvents. *Journal of Solution Chemistry* **1979,** *8*, 461-478.

(9) Evans, D. F.; Tominaga, T.; Davis, H. T. Tracer Diffusion in Polyatomic Liquids. *J. Chem. Phys.* **1981,** *74*, 1298-1305.

(10) Marrink, S.-J.; Berendsen, H. J. C. Simulation of Water Transport through a Lipid Membrane. *J. Phys. Chem.* **1994,** *98*, 4155-4168.

(11) Daldrop, J. O.; Kowalik, B. G.; Netz, R. R. External Potential Modifies Friction of Molecular Solutes in Water. *Phys. Rev. X* **2017,** *7*, 041065.

(12) Nagai, T.; Tsurumaki, S.; Urano, R.; Fujimoto, K.; Shinoda, W.; Okazaki, S. Position-Dependent Diffusion Constant of Molecules in Heterogeneous Systems as Evaluated by the Local Mean Squared Displacement. *J. Chem. Theory Comput.* **2020,** *16*, 7239-7254.

(13) Fujimoto, K.; Nagai, T.; Yamaguchi, T. Momentum Removal to Obtain the Position-Dependent Diffusion Constant in Constrained Molecular Dynamics Simulation. *J Comput Chem* **2021,** *42*, 2136-2144.

(14) Morgan, D.; Ferguson, L.; Scovazzo, P. Diffusivities of Gases in Room-Temperature Ionic Liquids: Data and Correlations Obtained Using a Lag-Time Technique. *Ind. Eng. Chem. Res.* **2005,** *44*, 4815-4823.

(15) Kaintz, A.; Baker, G.; Benesi, A.; Maroncelli, M. Solute Diffusion in Ionic Liquids, Nmr Measurements and Comparisons to Conventional Solvents. *J. Phys. Chem. B* **2013,** *117*, 11697-708.

(16) Araque, J. C.; Yadav, S. K.; Shadeck, M.; Maroncelli, M.; Margulis, C. J. How Is Diffusion of Neutral and Charged Tracers Related to the Structure and Dynamics of a Room-Temperature Ionic Liquid? Large Deviations from Stokes-Einstein Behavior Explained. *J. Phys. Chem. B* **2015,** *119*, 7015-29.

(17) Kimura, Y.; Kida, Y.; Matsushita, Y.; Yasaka, Y.; Ueno, M.; Takahashi, K. Universality of Viscosity Dependence of Translational Diffusion Coefficients of Carbon Monoxide, Diphenylacetylene, and Diphenylcyclopropenone in Ionic Liquids under Various Conditions. *J. Phys. Chem. B* **2015,** *119*, 8096-103.

(18) Canongia Lopes, J. N.; Padua, A. A. Nanostructural Organization in Ionic Liquids. *J. Phys. Chem. B* **2006,** *110*, 3330-5.

(19) Tomšič, M.; Bešter-Rogač, M.; Jamnik, A.; Kunz, W.; Touraud, D.; Bergmann, A.; Glatter, O. Nonionic Surfactant Brij 35 in Water and in Various Simple Alcohols: Structural Investigations by Small-Angle X-Ray Scattering and Dynamic Light Scattering. *J. Phys. Chem. B* **2004,** *108*, 7021-7032.

(20) Triolo, A.; Russina, O.; Bleif, H. J.; Di Cola, E. Nanoscale Segregation in Room Temperature Ionic Liquids. *J. Phys. Chem. B* **2007,** *111*, 4641-4.

(21) Russina, O.; Triolo, A. New Experimental Evidence Supporting the Mesoscopic Segregation Model in Room Temperature Ionic Liquids. *Faraday Discuss* **2012,** *154*, 97-109.

(22) Yamaguchi, T. Coupling between the Mesoscopic Dynamics and Shear Stress of a Room-Temperature Ionic Liquid. *Phys. Chem. Chem. Phys.* **2018,** *20*, 17809-17817.

(23) Allen, M. P.; Tildesley, D. J. *Computer Simulation of Liquids*. Clarendon Press: Oxford, 1987.

(24) Hansen, J.-P.; McDonald, I. R. *Theory of Simple Liquids*. 2nd ed.; London: Academic Press, 1986.

(25) Boon, J.-P.; Yip, S. *Molecular Hydrodynamics*. Dover: New York, 1991.

(26) Yamaguchi, T.; Matsuoka, T.; Koda, S. Molecular Dynamics Simulation Study on the Transient Response of Solvation Structure During the Translational Diffusion of Solute. *J. Chem. Phys.* **2005,** *122*, 14512.

(27) Zhong, X.; Liu, Z.; Cao, D. Improved Classical United-Atom Force Field for Imidazolium-Based Ionic Liquids: Tetrafluoroborate, Hexafluorophosphate, Methylsulfate, Trifluoromethylsulfonate, Acetate, Trifluoroacetate, and Bis(Trifluoromethylsulfonyl)Amide. *J. Phys. Chem. B* **2011,** *115*, 10027-40.

(28) Verlet, L.; Weis, J.-J. Perturbation Theory for the Thermodynamic Properties of Simple Liquids. *Mol. Phys.* **1972,** *24*, 1013-1024.

(29) Hess, B.; Bekker, H.; Berendsen, H. J. C.; Fraaije, J. G. E. M. Lincs: A Linear Constraint Solver for Molecular Simulations. *J. Comput. Chem.* **1997,** *18*, 1463-1472.

(30) Abraham, M. J.; Murtola, T.; Schulz, R.; Páll, S.; Smith, J. C.; Hess, B.; Lindahl, E. Gromacs: High Performance Molecular Simulations through Multi-Level Parallelism from Laptops to Supercomputers. *SoftwareX* **2015,** *1-2*, 19-25.

(31) Martin, M. G.; Siepmann, J. I. Transferable Potentials for Phase Equilibria. 1. United-Atom Description Ofn-Alkanes. *J. Phys. Chem. B* **1998,** *102*, 2569-2577.

(32) Chen, B.; Potoff, J. J.; Siepmann, J. I. Monte Carlo Calculations for Alcohols and Their Mixtures with Alkanes. Transferable Potentials for Phase Equilibria. 5. United-Atom Description of Primary, Secondary, and Tertiary Alcohols. *J. Phys. Chem. B* **2001,** *105*, 3093-3104.

(33) Kashyap, H. K.; Hettige, J. J.; Annapureddy, H. V.; Margulis, C. J. Saxs Anti-Peaks Reveal the Length-Scales of Dual Positive-Negative and Polar-Apolar Ordering in Room-Temperature Ionic Liquids. *Chem. Commun.* **2012,** *48*, 5103-5.

(34) Yeh, I.-C.; Hummer, G. System-Size Dependence of Diffusion Coefficients and Viscosities from Molecular Dynamics Simulations with Periodic Boundary Conditions. *J. Phys. Chem. B* **2004,** *108*, 15873-15879.

(35) Araque, J. C.; Margulis, C. J. In an Ionic Liquid, High Local Friction Is Determined by the Proximity to the Charge Network. *J. Chem. Phys.* **2018,** *149*, 144503.

TOC Graphic